Supporting Information for

Molecularly anchoring TPE-PDMS micro-dots for rupture-free and high-fidelity deformation mapping

Wenbo Wang,[ab] Zhihao Zhao,[c] Xiaohan Sun,[c] Lingyun Xu,[c] Zhao Wang,[*a] Xiangyu Jiang[*d] and Shutao Wang[ab]

[a] Laboratory of Bio-inspired Smart Interface Science, Technical Institute of Physics and Chemistry, Chinese Academy of Sciences, Beijing 100190, China.
[b] University of Chinese Academy of Sciences, Beijing 101408, China.
[c] School of Chemistry, Beihang University, Beijing 100191, China.
[d] International Research Institute for Multidisciplinary Science, Beihang University, Beijing 100191, China.

***Corresponding author.**

E-mail address: wangzhao@mail.ipc.ac.cn; jiangxy@buaa.edu.cn

Table of contents

1. Materials and chemicals

Silicone elastomer kit (SYLGARD^{TM} 184), aminopropyl terminated polydimethyl siloxane (Macklin), 4-(1,2,2-triphenylvinyl)benzaldehyde (Macklin), 1H,1H,2H,2H-Perfluorooctyltriethoxysilane (Sigma Aldrich), tetraphenylethylene (Macklin), and ethanol (Shanghai test) were used directly without further purification. Solvents used for syntheses and measurements were of analytical grade unless stated otherwise. Deionized water was purified using a Milli-Q system.

2. Characterizations

Optical microscopy images were observed using an optical microscope (LEICA DM 2700M). UV-vis absorption spectra were acquired on a UV2600 spectrometer (Shimadzu). The macroscopic adhesion strength was measured using an M5-2 dynamometer (Mark-10 Corporation). The variation of fluorescence intensity was observed through confocal laser scanning microscopy (Nikon-ARsiMP-LSM-Kit-Legend Elite-USX, Nikon, Japan). The dynamic contact angles (CA) of water droplets on the samples (1 × 1 cm^2) were recorded by the OCA-20 machine (Dataphysics Germany). The volume of water droplets was set as 2 μL. Infrared (IR) spectra were recorded using a Varian 3100 FT-IR. Optical microscopy images were observed by an optical microscope (LEICA DM 2700M). Atomic Force Microscopy (Bruker MultiMode 8 Atomic Force Microscope). Silicon wafers with micro-column structure (Institute of Micro-Nanoelectronics, Peking University). Scanning electron microscope (S-4800, JEOL). Fluorescence confocal microscope (Olympus FV100).

3. Synthesis of TPE-PDMS

A mixture of 100 mg (0.277 mmol) of 4-(1,2,2-triphenylvinyl)benzaldehyde (TPE-CHO) (M_w: 360.455) and 118.15-125.1 mg (0.139 mmol) of amine-terminated PDMS (PDMS-NH_2) (M_w: 850-900) in 20 mL of ethanol (HPLC grade) was heated under reflux at 100°C for 6 hours. After the reaction mixture was cooled to room temperature, sodium borohydride ($NaBH_4$, 52.3 mg, 1.38 mmol) was added slowly under ice-bath cooling. The mixture was then stirred at this temperature for 12 hours, yielding a white solution.[1-2] Deionized water was added dropwise to the white solution, resulting in the formation of white flocculent precipitate. After thorough stirring, an additional 10 drops of deionized water were added. The white precipitate was removed by suction filtration, and the ethanol solvent was evaporated under reduced pressure to give a white viscous product. The product was dissolved in dichloromethane (CH_2Cl_2) and extracted three times with saturated NaCl aqueous solution. The lower organic layer was collected and dried over an excess amount of anhydrous Na_2SO_4 for 30 minutes to remove residual water. The supernatant was then collected, and CH_2Cl_2 was removed by rotary evaporation to yield the final product as a pale yellow solid, denoted as TPE-PDMS, yield: ≈80%.

4. Fabrication of TPE-PDMS dot arrays on PDMS

4.1 Preparation of flexible PDMS elastomer substrates

10 g silicone elastomer base and 1 g silicone elastomer curing agent were mixed thoroughly by mechanical stirring for 10 minutes to achieve a homogeneous mixture. The mixture was then placed under a vacuum environment to remove air bubbles. After complete bubble removal, the bubble-free, viscous, and transparent mixture was poured onto a flat and clean glass substrate measuring 10 cm × 10 cm. A polytetrafluoroethylene (PTFE) ring spacer with a thickness of 0.5 cm was placed around the edges of the glass substrate. Another glass slide of the same dimension was carefully placed on top, ensuring no bubbles were trapped between the mixture and the glass during this process. The two glass slides were secured with binder clips and transferred into an oven set at 80°C for thermal curing over 2 hours. After curing, the assembly was cooled to room temperature. Finally, the PTFE spacer and glass substrates were removed to obtain a silicone-based elastomer sheet with a thickness of 0.5 cm.

4.2 Surface Modification of Silicon Wafer

A silicon wafer (1 cm × 1 cm) with a micropillar array structure (pillar diameter: 10 μm, spacing: 3 μm, height: 10 μm) was processed using photolithography and deep reactive ion etching (DRIE) with a direct laser writing system (Fig. S1, ESI†). The silicon wafer was immersed in piranha solution and cleaned at 80°C for 0.5 hours to remove surface impurities. Subsequently, the tops of the micropillars were protected with an SU-8 layer and the low-surface-energy perfluorosilane was evaporated onto the unprotected surfaces. Finally, after the SU-8 layer was removed, a micropillar template with asymmetric wettability was obtained.

4.3 Sandwich Structure Assembly

The obtained 20 mg TPE-PDMS was dissolved in 1 mL anhydrous ethanol and stirred thoroughly at room temperature to obtain a clear and transparent TPE-PDMS solution with a concentration of 20 $mg \cdot mL^{-1}$. A 0.5 cm thick PDMS film substrate was cut into a spindle shape using a spindle-shaped mold and then treated with plasma for 8 minutes in a plasma cleaner. 10 μL of the TPE-PDMS solution was dropped onto the silicon wafer with asymmetric wettability. The non-swelling of PDMS in ethanol ensures the stable growth of the TPE-PDMS arrays (Fig. S2, ESI†). The PDMS film was then placed over the silicon wafer, followed by covering with a glass slide. The silicon wafer and the glass slide below it was clamped together with a clip to ensure close contact between the silicon wafer and the PDMS film, maintaining structural stability without movement during solvent evaporation. The difference in wettability between the two substrates causes TPE-PDMS to undergo preferential de-wetting on the PDMS surface (Fig. S3, ESI†). As the solvent gradually evaporated, a hemispherical dot array structure formed on the PDMS substrate.

Additionally, the viscosity of the synthesized TPE-PDMS increases with the molecular weight of PDMS (Figure S4). As shown in Figure S5, when the molecular weight of TPE-PDMS is low (500 $g \cdot mol^{-1}$), the low viscosity leads to a rapid dewetting process, resulting in micro-dot arrays with small sizes and irregular shapes. At very

high molecular weights (1500 and 3000 $g \cdot mol^{-1}$), the solution becomes highly viscous, hindering the dewetting process of the liquid bridges and preventing the formation of well-structured microlattices; instead, a thick adhesive layer is formed. In contrast, TPE-PDMS with a molecular weight of 850 $g \cdot mol^{-1}$ produces micro-dot arrays with regular shapes and uniform sizes. Therefore, TPE-PDMS (with PDMS molecular weight of 850-900 $g \cdot mol^{-1}$) was selected for subsequent experiments.

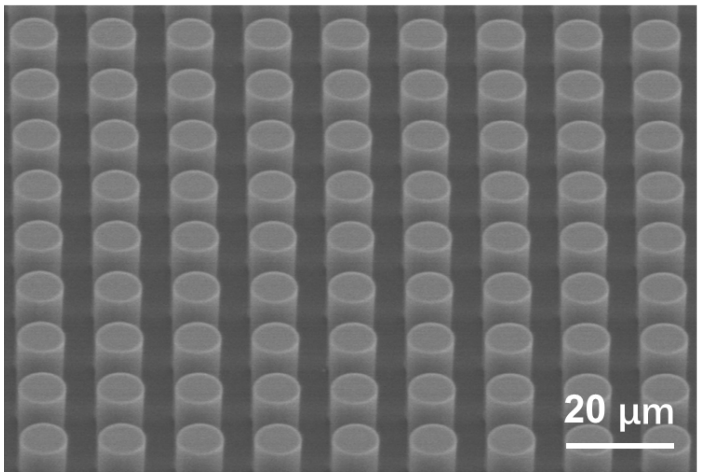

Figure S1. SEM image of micropillar-structured template (pillar diameter: 10 µm, spacing: 3 µm, height: 10 µm).

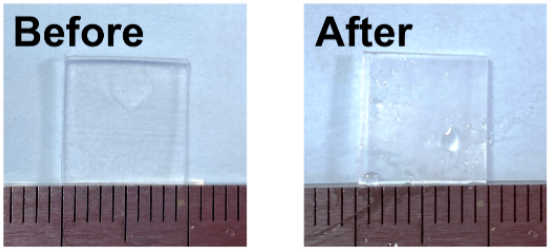

Figure S2. Optical images of the PDMS substrate before and after ethanol immersion, demonstrating its non-swelling behavior.

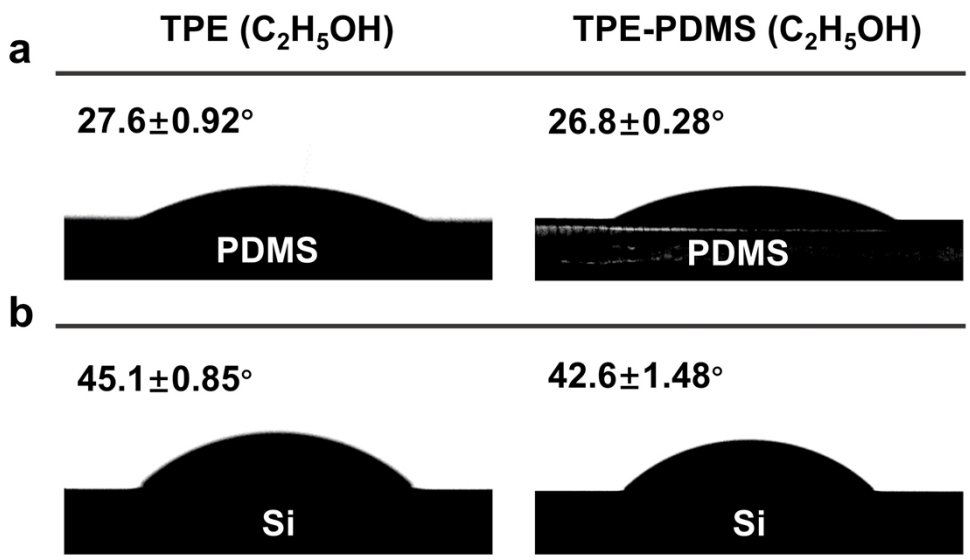

Figure S3. Contact angles of TPE/ethanol and TPE-PDMS/ethanol solutions. (a) A low contact angle (26.8 ± 0.28°) on PDMS surface and (b) a higher contact angle (42.6 ± 1.48°) on silicon surface.

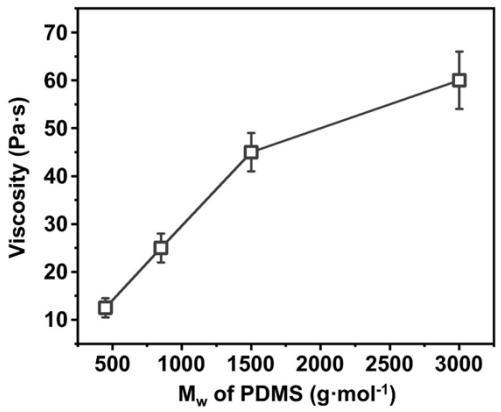

Figure S4. The viscosity of TPE-PDMS increases as the molecular weight (M_w) of PDMS increases.

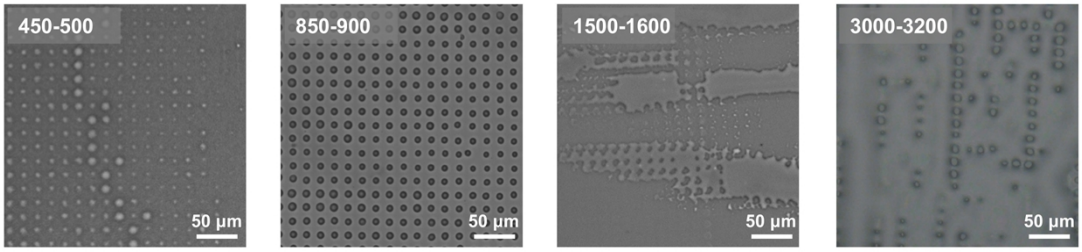

Figure S5. Optical microscopy images of TPE-PDMS micro-dots with increasing PDMS molecular weight. The most complete and orderly dot array morphology is observed at 850-900 $g \cdot mol^{-1}$.

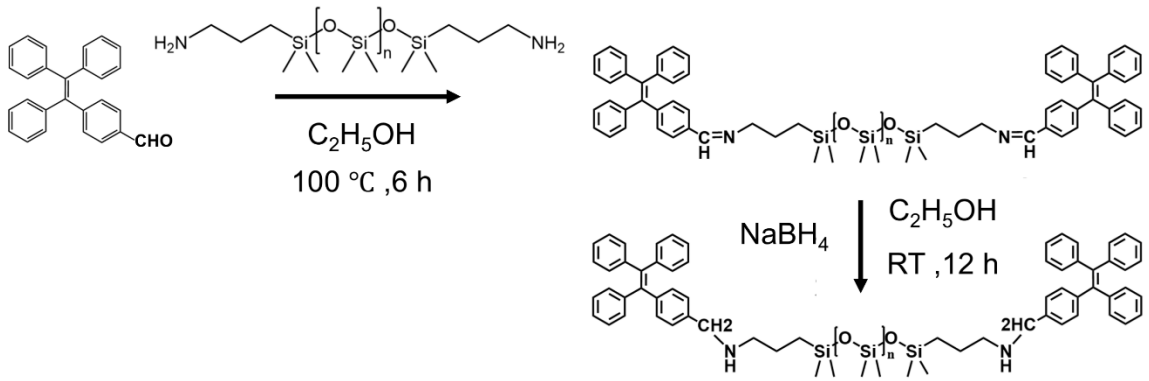

Figure S6. Synthesis procedures of TPE-PDMS. TPE-PDMS were synthesized through aldehyde-ammonia condensation reaction between TPE-CHO and PDMS-NH_2.

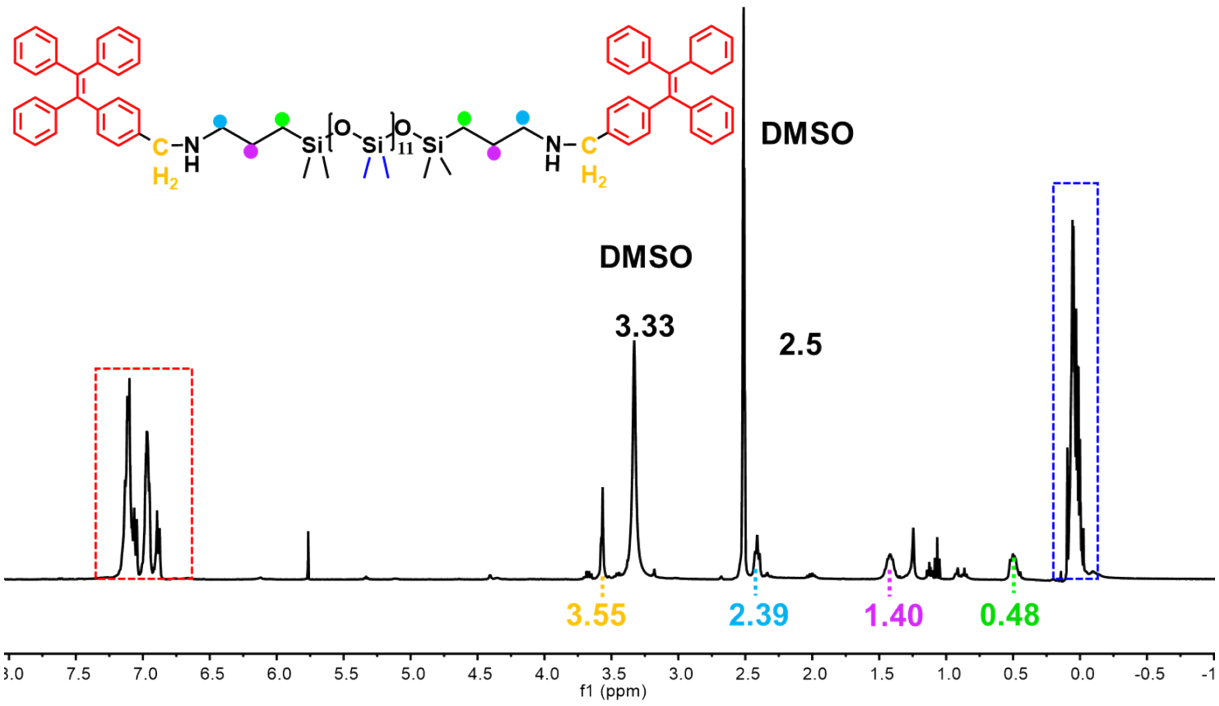

Figure S7. TPE-PDMS. ^{1}H NMR (400 MHz, DMSO-d_6): δ 7.12 (q, J = 6.0, 3.6 Hz, 14H), 6.91 (m, 3H), 6.89 (dd, J = 15.8, 9.6 Hz, 2H), 3.55 (d, J = 5.5 Hz, 2H), 2.39 (q, J = 7.1, 6.0 Hz, 2H), 1.40 (s, 2H), 0.48 (m, 2H), 0.06 (d, J = 5.4 Hz).

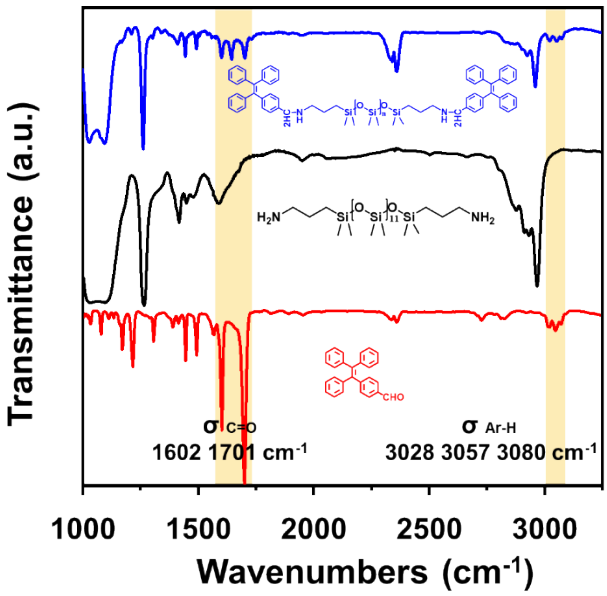

Figure S8. The FT-IR spectra comparison of TPE-CHO and TPE-PDMS. The weakening of the characteristic aldehyde peaks at 1701 and 1602 cm^{-1} confirms the successful aldehyde-amine condensation reaction.

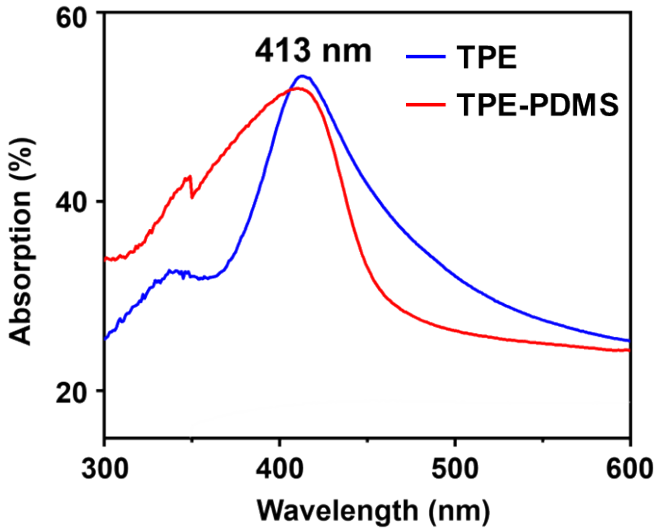

Figure S9. The UV-Vis absorption spectra of TPE and TPE-PDMS show that their absorption peaks remain around 413 nm after the grafting of the PDMS segment.

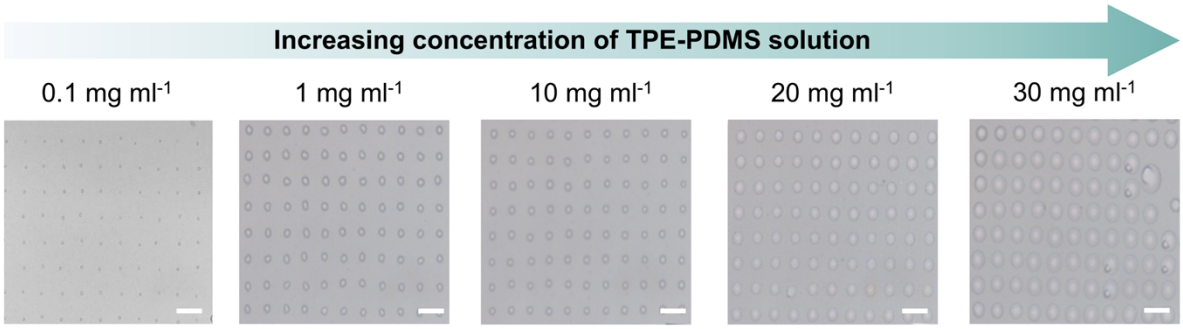

Figure S10. Optical photographs of the TPE-PDMS dot arrays show that the array size increases with the solution concentration. Scale bars: 20 μm.

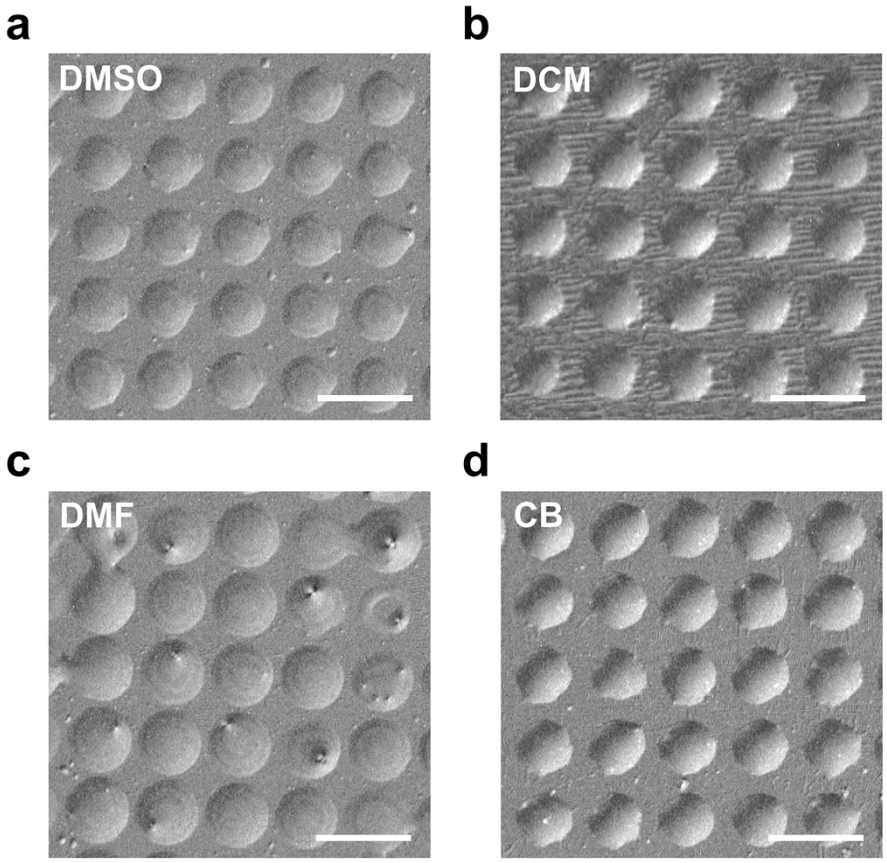

Figure S11. Confocal microscopy images of TPE-PDMS dot arrays prepared with different solvent including (a) dimethyl sulfoxide (DMSO), (b) dichloromethane (DCM), (c) N,N-dimethylformamide (DMF), (d) chlorobenzene (CB). Scale bars: 20 μm.

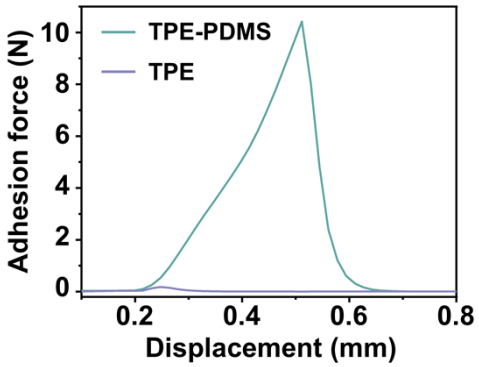

Figure S12. Force-displacement curves of TPE-PDMS and TPE. TPE-PDMS exhibits stronger adhesion strength.

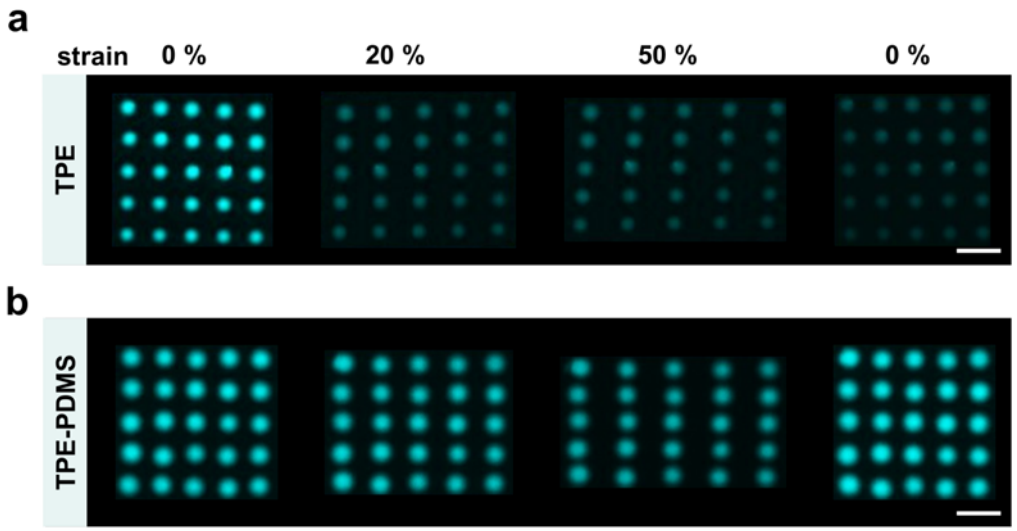

Figure S13. Comparison of fluorescence stability between (a) TPE and (b) TPE-PDMS under prolonged UV irradiation. As the strain increases, the fluorescence intensity of the TPE arrays significantly decreases and cannot be restored, while the fluorescence intensity of the TPE-PDMS arrasy gradually decreases and can return to the initial intensity. Scale bars: 20 μm.

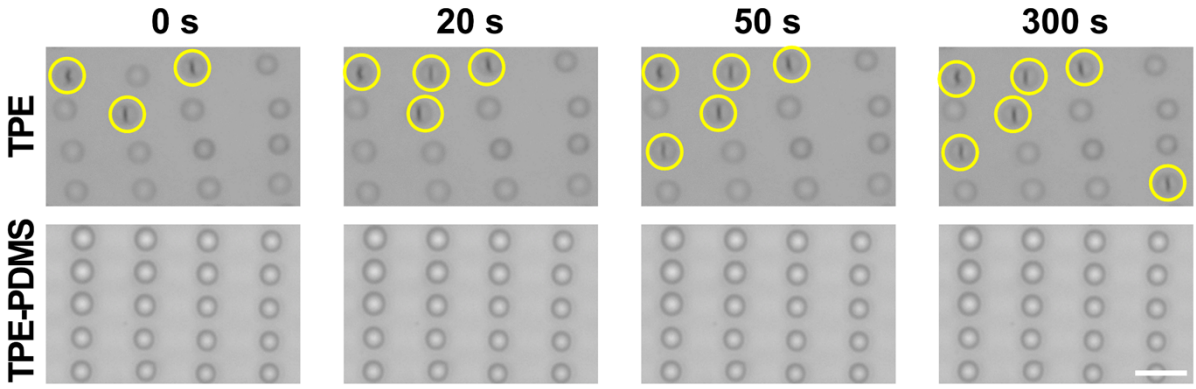

Figure S14. Comparison of array morphology between TPE and TPE-PDMS under continuous stretching (0-300 s). Structural failure occurs in the TPE arrays over time, while the TPE-PDMS arrays remain intact. Scale bars: 20 μm.

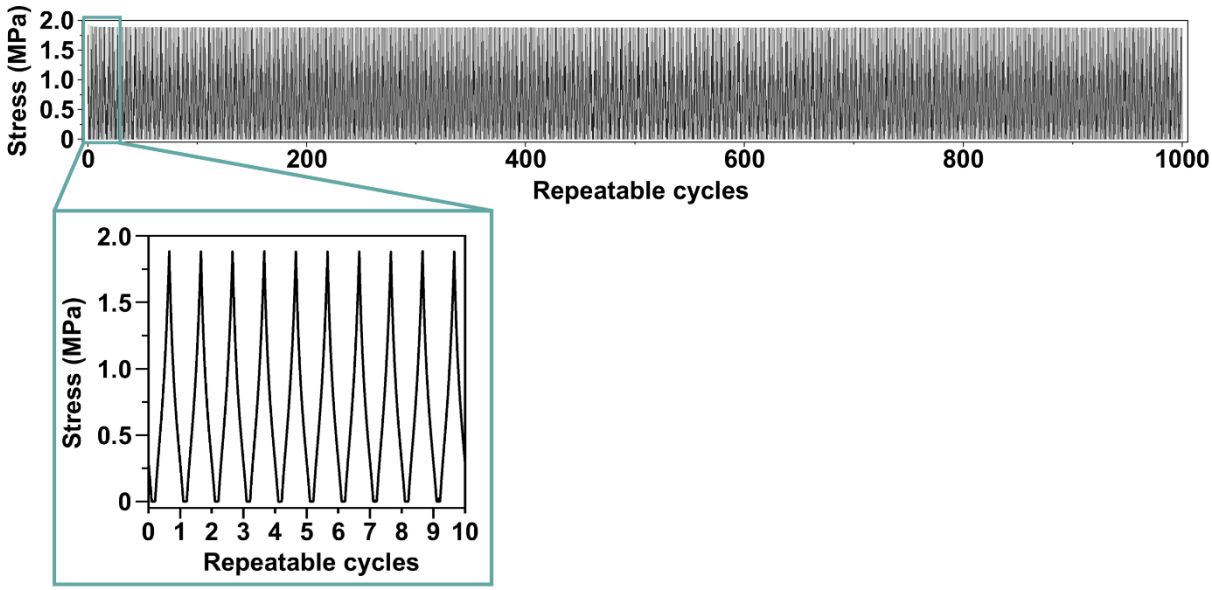

Figure S15. 1000 cyclic stretching test of the PDMS substrate with TPE-PDMS arrays.

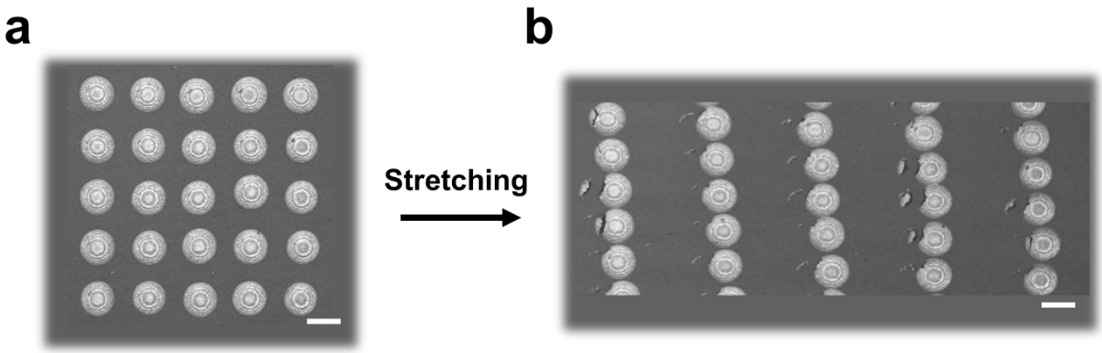

Figure S16. Confocal microscopy images of TPE dot arrays before and after stretching. The array topographies remain essentially unchanged but exhibit localized fracture as a result of weak molecule-substrate adhesion. Scale bars: 10 μm.

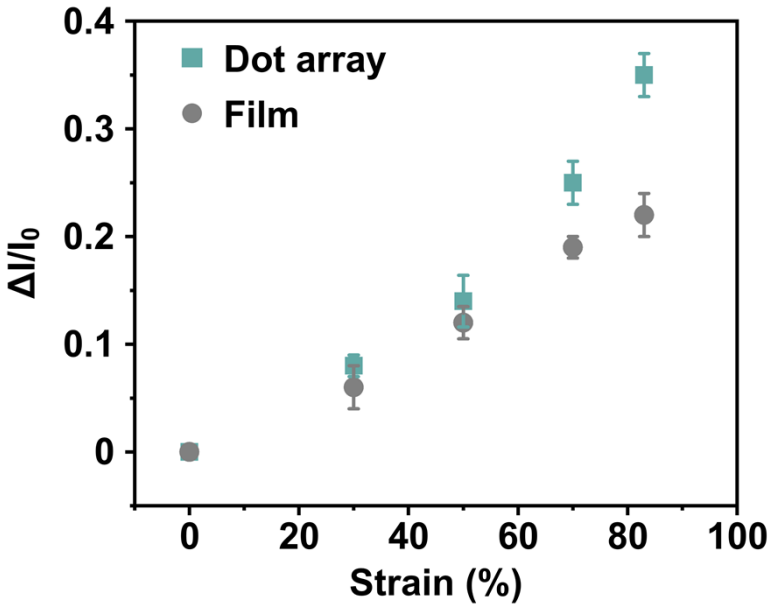

Figure S17. Relative variations of the fluorescent intensity ($\Delta I/I_0$) of TPE-PDMS dot arrays and TPE-PDMS film. TPE-PDMS dot arrays exhibit higher sensitivity.

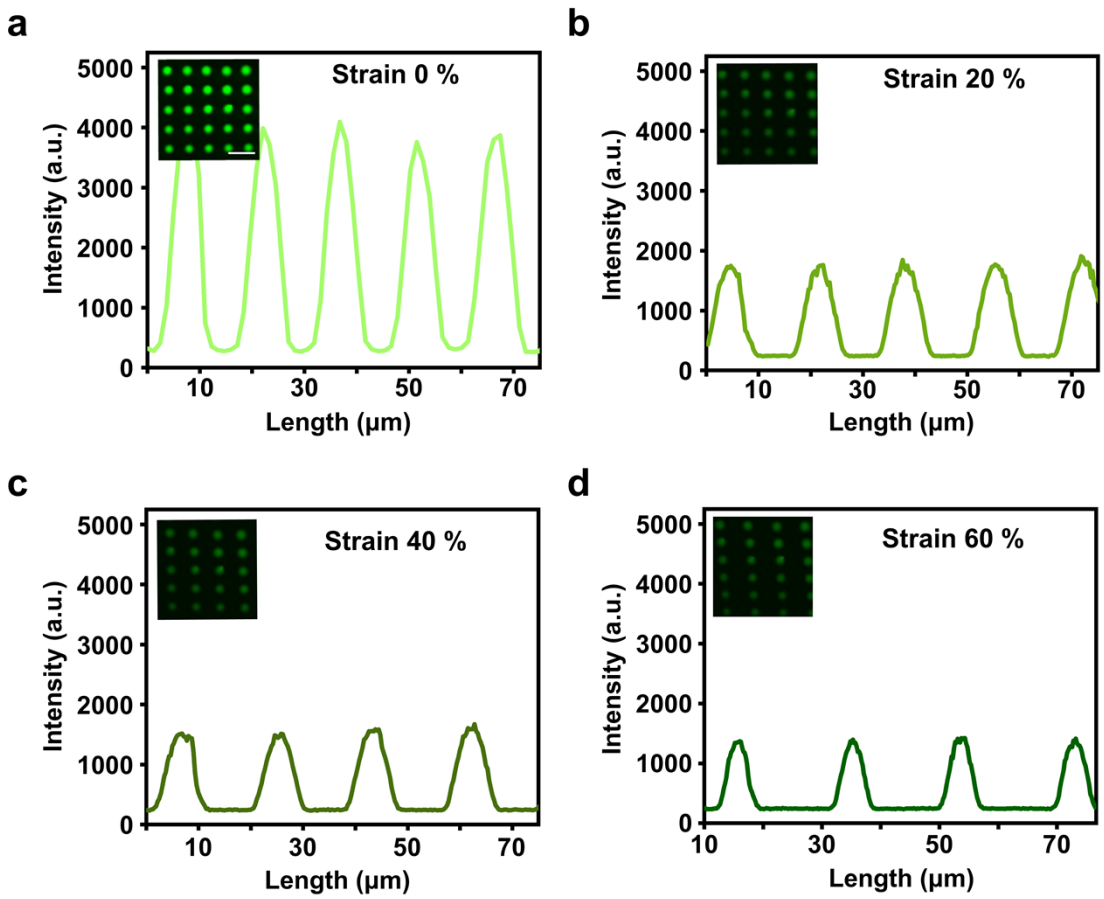

Figure S18. In situ real-time fluorescence intensity of the TPE dot arrays during the stretching of the flexible substrate to strains of (a) 0%, (b) 20%, (c) 40%, and (d) 60%. Inset: laser confocal photographs of the TPE-PDMS dot arrays (scale bars: 20 μm).

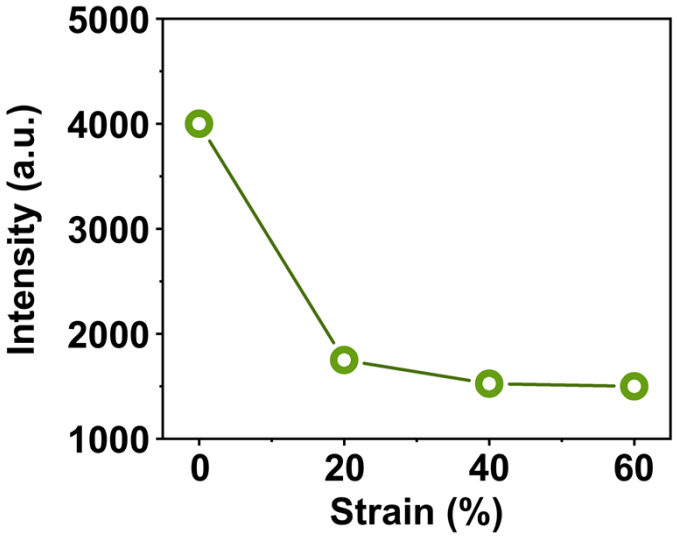

Figure S19. Fluorescence intensity of TPE dot arrays under different strain conditions. The fluorescence intensity first drops sharply and then remains constant.

References:

1. A. F. AbdelMagid, K. G. Carson, B. D. Harris, C. A. Maryanoff, R. D. Shah, *J. Org. Chem.* **1996**, 61, 3849.

2. E. R. L. Brisson, Z. Y. Xiao, G. V. Franks, L. A. Connal, *Biomacromolecules* **2017**, 18, 272.